Scientific Research Publishing

Applied Mathematics, 2026, 17(1), 54-73
https://www.scirp.org/journal/am
ISSN Online: 2152-7393
ISSN Print: 2152-7385

# Solar Energy Driven Convective Transport Model in the Troposphere

**George Danko**

Mackay School of Earth Science and Engineering, University of Nevada, Reno, NV, USA
Email: danko@unr.edu

**How to cite this paper:** Danko, G. (2026) Solar Energy Driven Convective Transport Model in the Troposphere. *Applied Mathematics*, **17**, 54-73.
https://doi.org/10.4236/am.2026.171005

**Received:** December 15, 2025
**Accepted:** January 25, 2026
**Published:** January 28, 2026



## Abstract

Vertical, convective, thermal energy transport is examined outside the box of microscale turbulent dispersion or unstable air parcels driven by energy pockets along adiabatic trajectories. The focus is the mathematical model of the dormant, very recently discovered Carnot Compression-Expansion (CCE) cells residing in the atmosphere stratified by gravity, and the vertical gradients of pressure, temperature, and density. Two cases are analyzed in search for interactions between the CCE cells and the natural processes in the atmosphere, such as 1) the mixing-driving capacity of the horizontal wind, energizing the Carnot processes; and 2) the driver of the thermal expansion and contraction of the troposphere by periodic solar heating and self-radiation cooling of the ground. The second process is self-generated and shows a stronger vertical energy transport than the first in the troposphere, even without horizontal wind enhancement. The spatially uneven heating and cooling effects from surface and cloud variations can be conveniently analyzed with a single-column system if no net horizontal, mesoscale driving gradients are present. Conclusions are discussed from a real-world example and a numerical model.

## Keywords

Carnot Compression-Expansion (CCE) Cells, Vertical Energy Transport, Stratified Atmosphere, Mathematical Modeling, Atmospheric Thermodynamics

## 1. Introduction

The focus of the presented work is to re-examine and generalize the vertical, convective, thermal energy transport in the troposphere (TR) and stratosphere (ST) of the Earth. Energy transport network models applicable to atmospheric processes are described in a previous publication [1] for all common forms and mech-

anism including heat conduction, convection, diffusion, dispersion, advection, radiation, and phase change. An example was presented for solving the transport of heat and moisture components in the atmosphere in their temporal evolution in a fixed volume over a continuous, three-month time interval to examine the validity of the mathematical models against measured weather data within a large control volume around a single weather monitoring station [1].

The existence of spontaneous thermal energy transport by Carnot Compression-Expansion (CCE) cells was discovered in the TR zone [1]. It is a connected series of cell-type, vertical transport systems with cyclic advection and convection, activated and powered by the horizontal wind. As shown, significant rates of thermal energy can be moved by the series of CCE cells in the vertical direction across the compressible air in vertically stratified temperature and barometric pressure field under gravitational force. The CCE cell is a new, purely convective, "heat engine" mechanism, capable of converting horizontal, large-eddy kinetic wind energy to vertical energy transport, without employing the microscale eddy diffusivity concept.

The structure of the study is as follows. After a brief overview of vertical convection in TR, a continued analysis beyond [1] will be provided to explain the components of vertical thermal energy transport based on the cyclic compression-expansion mechanisms in vertical direction without assuming net vertical mass transport in the air in a single column. Two possible models will be explained to show the cases where net zero vertical mass transport can be stipulated in a Representative Element Volume (REV) in TR by two basic hypotheses (H1 and H2) and two theorems (T1 and T2). The two CCE models will be then defined and numerically analyzed for their strength in vertical energy flux, as a continuation of the numerical example presented in [1].

### 1.1. Overview of the Convective Vertical Heat and Mass Transport in the Atmosphere

The present work re-examines and generalizes the vertical thermal energy transport by the CCE concept in the TR zone. The heat and mass fluxes in the boundary layer (BL) over the ground surface is governed the "laws of the wall," dealt with extensively in boundary layer theory [2] [3]. Atmospheric scientists, following Molin and Obukhov [4]-[6], adopted the eddy diffusivity and turbulent dissipation due to large-eddy mixing and fluctuations in the lowest layers of TR with the vertical, turbulent heat flux, $\omega'T'$, and mass flux, $u'\omega'$, expressed as covariances of the velocities and the temperature components, $\omega'$, $T'$ and $u'$. In Obukhov's concept, these components were assumed to be constant with elevation in BL. Weather science does not use the surface heat and mass transport coefficient concepts for laminar or turbulent, stable, or unstable BC layers over the ground, missing the convenience of an intermittent, measurable, transport model component, described and used in [1]. The BC layer is a very small, but important part of TR, assumed to be below the elevation of the monitored point

for the air temperature, $Ta$. Two other areas above the BL have active, convective vertical transport: 1) the zone of TR between the elevation of the measured point of $Ta$, and below the height of the lower edge of the tropopause; and 2) the zone above it, between the elevation of the lower edge (umbrella layer) of ST and below the height of the upper edge of the tropopause layer at some 20 km elevation.

The zone of 1) in TR is often handled with the same model as of the BL, expanding Obukhov's concept, and increasing the applicable height of a BL model, high into the atmosphere [7]. Convective transport (driven by gradients in a strict definition) is broadly defined in atmospheric science interchangeably with advection (that is driven, strictly, by advective velocity in the transport literature, especially in hydrology). Vertical transport of thermal energy and mass by convection uses the Convective Available Potential Energy (CAPE) parameter in mathematical models, as well as in observational explanations of cloud formations and storms, briefly reviewed in [1]. CAPE is used to explain the formation of cumulus clouds and thunderstorm clouds, as if the driving energy to lift a lump of mass in TR were along an adiabatic transport process in TR. Assuming mechanical energy balance along an adiabatic, instead of a constant compression index trajectory, $n$, ignores the combined effects of changing pressure, elevation, temperature and the loss of energy due to friction loss, explained in [1]. Using CAPE as the driving force for vertical lift of air disagrees with the conservation of the mechanical energy along a movement trajectory of constant $n$ for a lump of mass in TR as it was shown in [1]. Empirical adjustments are needed to alleviate the conceptual weakness of using CAPE as the maximum energy available to an ascending parcel in dry or moist-air convection. Multiple types of CAPE are described in the literature, such as one for downdraft (DCAPE), surface based (SBCAPE), mixed layer or mean layer CAPE (MLCAPE), most unstable or maximum usable (MUCAPE), or normalized (NCAPE), serving the needs for adjustments.

### 1.2. The Basic Hypotheses and Theorems for CCE Models in the Atmosphere

Hypothesis 1 (H1): Under a quiet fair-weather condition, zero horizontal gradients for energy, momentum and mass flux define a useful subclass of weather processes in the TR. The H1 is an assumption that such a subclass is not an empty set in the ST and there exists tangible time periods (hours, days, or weeks) during which no significant, horizontal change in air temperature, barometric pressure, horizontal air velocity, or other properties are experienced within the representative element volume (REV) defined as 10 km × 10 km × 10 km [1]. H1 is intuitive as more than one monitoring station is needed to experimentally prove it. However, the spatially sparse set of monitoring stations for meaningful and useful weather reporting assume that each data point has a long, horizontal range of validity, with negligibly changing gradients, supporting H1.

Hypothesis 2, (H2). The single column solver (SCS) model for its REV volume to represent the STR must have horizontally zero net air mass flux exchange with

its surrounding volumes in the atmosphere. H2 is a simplifying stipulation for the applicability of the SCS model, at least for time periods, confirmed by H1.

Theorem 1 (T1): Assuming the validity of H1 and H2, the total thermodynamic (TT) and the total mechanical (TM) energy must be both conserved within the REV volume of the STR with zero horizontal gain or loss components.

The proof of T1 is trivial, following the conservation laws for energy and the teaching from the first law thermodynamics. The REV volume is assumed to be closed by the insulating boundaries amid horizontally zero energy gradients on the vertical planes.

Theorem 2 (T2): Assuming the validity of H1 and H2, the total air mass within the REV volume of the STR is not affected by mass fluxes of the horizontal wind or on the ground wall.

The proof of T2 comes from the mass conservation law for a closed volume due to zero gradient-(that is, insulating) boundaries in the vertical planes and zero vertical air flow across the ground wall. The only open boundary for air mass to flow across is at the TR upper horizontal layer, which allows for vertical, in-and-out breathing or diffusion-dispersion mass transport with the tropopause layer in the ST.

## 2. Thermodynamic and Mechanical Energy Transport in a Network Branch

The CCE process assumes changes with time and location between two points. Network branches between any two points in the TR or ST are pictured as series of thermodynamic energy (TDE) transport cells in the atmospheric air. The TDE transport includes thermal ( $H$ ) and mechanical work ( $W$ ) components. The $H$ component may move air indirectly by thermal expansion or compression. The shaft energy component, $W_s$, may be a positive, direct driver by a pump, fan, or velocity blower, or a negative, direct drag on the air movement by friction resistance $W_\tau$.

It is straightforward to separate the $H$ and the $W$ components in the TDE system by assuming a network along a possible streamline of air motion between two points, and a TDE transport process with a compression index, $n$, that can be iteratively refined by resolving the TDE, together with the mass, and momentum balance equations [8]. Between two points along any $n$ = constant streamline, the total differential of the Bernoulli-type mechanical energy components of a lump of mass can be written (in two preferred forms) by formal expansion and the gas law for $n \neq 1$ as:

$$\begin{aligned} d\left(\frac{P}{\rho}+g\cdot z+\frac{v^2}{2}\right) &= d\left[\left(\frac{n}{n-1}\right)\frac{P}{\rho}-\left(\frac{1}{n-1}\right)\frac{P}{\rho}+g\cdot z+\frac{v^2}{2}\right] \\ &= d\left[\left(\frac{n}{n-1}\right)R\cdot T+g\cdot z+\frac{v^2}{2}\right]-\left[\left(\frac{1}{n-1}\right)R\cdot T\right] \end{aligned} \tag{1}$$

It is shown in [8] that $n$ is indeed the compression index for a compressible fluid, satisfying the definition of $\frac{p}{\varrho^n}=\text{constant}$ along a streamline movement.

The first term on the far right side of (1) represents the total change of the mechanical energy along a $ds$ streamline section and in $dt$ time. The second term on the right side of (1) is the change of thermal energy associated with the polytropic expansion or compression process during the movement of a lump of unit mass along a $ds$ section. The changes in pressure ($P$), density ($\rho$), elevation ($z$), velocity ($v$), and temperature ($T$) are all taken along the $ds$ section of a streamline of the movement of unit mass.

For $n=1$, the process is isothermal, defined by $dT=0$, giving $\left(\frac{n}{n-1}\right)R\cdot T=\infty\cdot 0$ that can be resolved as an undetermined product as $R\cdot T_1\cdot\ln\left(\frac{P_2}{P_1}\right)$ where the flow is from point ($P_1,T_1$), to point ($P_2,T_2$), along $ds$.

Therefore, the mechanical energy conservation equation may be written for a differential, or a finite-difference change along a streamline of $n$ compression index as:

$$d\left[\left(\frac{n}{n-1}\right)R\cdot T+g\cdot z+\frac{v^2}{2}\right]=d\left(W_s-W_\tau\right)\quad\text{for}\quad n\neq 1 \tag{2a}$$

$$\left[R\cdot T_1\cdot\ln\left(\frac{P_2}{P_1}\right)+g\cdot\left(z_2-z_1\right)+\frac{v_2^2-v_1^2}{2}\right]=d\left(W_s-W_\tau\right),\ \text{for}\quad n=1 \tag{2b}$$

where $W_s$ is energy generation by "shaft" input work, and $W_\tau$ is dissipation by friction loss. The compression index, *n*, between points 1 and 2 along the assumed streamline section is always:

$$n=\frac{\ln\left(\frac{P_2}{P_1}\right)}{\ln\left(\frac{P_2}{P_1}\right)-\ln\left(\frac{T_2}{T_1}\right)} \tag{3}$$

Another special case in addition to the isothermal is the adiabatic (or isentropic) compression, when $n=\kappa=Cp/Cv$. Both isothermal and adiabatic cases, together with the general, polytropic (diabatic) compression index are used in the model of a single CCE cell on a network branch, introduced in [1].

It is notable that the compression index in the TR atmosphere in a real-world example in [1] over a 3-month period always stayed in the closed interval between the isothermal and adiabatic cases, $1<n<\kappa$ in the SCS model. The expectation is that Equation (2a) will seldomly encounter a singularity problem in other TR examples to force switching to (2b) for the energy conservation model.

The air temperature is assumed to be linear between the two end points of a network branch. For a baseline SCS model, one branch is used to connect the close-to-ground point at $Ta$ the temperature sensor to the top of TR at $Tu$ umbrella temperature:

$$T\left(z\right)=Ta+\frac{Tu-Ta}{L}\cdot z=Ta+alr\cdot z \tag{4}$$

The $alr$ is the time-dependent, but constant lapse rate along the elevation, $z$, measured from the ground's level at the measurement point of the air temperature, $Ta$.

The compression index, $n$, can be evaluated from two points of measured weather data along an expected streamline, ($P_1, T_1$), and ($P_2, T_2$), using Equation (3). The best start for SCS model definition is when monitored data are available from two points simultaneously at different elevations for the direct evaluation of $n$. Otherwise, as happened in the example in [1], the missing element must be resolved by model tryouts. For the case of lacking barometric pressure at higher than at surface elevation, the hydrostatic law was used in [1], recalled for convenience as:

$$\frac{dP(z)}{dz} = -\frac{(g - dg)\cdot P(z)}{R\cdot(Ta + alr\cdot z)}, \tag{5}$$

where $P$, $g$, $dg$, $R$, $Ta$, and $alr$ are barometric pressure, gravitational constant, hydrostatic defect (similar to the "defect" term, $\chi$, introduced by Dutton [9]), gas constant for air, air temperature close to the ground wall, temperature lapse rate, respectively.

The hydrothermal defect is expressed as $dg = \frac{g\cdot dPt}{\bar{P}}$, a function of $dPt$ that is the added mechanical energy to the total kinetic energy of the single column in the TR. The mechanical energy change in vertical streamline direction, $dPt$, is the difference between energy generation, $dW_s$, and dissipation, $dW_\tau$, defined by the integral of the kinetic energy of the horizontal, streamline-directional wind component:

$$dPt = d\left(W_s - W_\tau\right) = C_1\int_0^{Dz} v(z)_s^2\, dz - C_2\int_0^{Dz} v(z)_s^2\, dz \tag{6}$$

The $C_1$, and $C_2$ coefficients (estimated first and iteratively refined during SCS model solution) express the differentially available, vertical, streamline-directional energy generation, $dW_s = C_1\int v(z)_s^2\, dz$, and the energy dissipation components from the integral of the horizontal kinetic energy of the airflow. The horizontal component of the streamline velocity of the air, $v(z)_s$, may be known close to the surface at $z = 0$ from a weather monitoring station; and from velocity sounding data along elevation $z$; or at least a single-point wind velocity from satellite data at the upper edge of TR at $z = Dz$. Linear interpolation of the horizontal air velocity component may be used between known points along the elevation in TR [1]. The vertically distributed, differential, net kinetic energy change in (6) may be positive ($dW_s > dW_\tau$) or negative ($dW_s < dW_\tau$) due to the existence or lack of horizontal, mesoscale or trade wind, expressed by the $C_1$, and $C_2$ coefficients.

For each hourly time index, $i$, the $n_i$ compression index can be calculated from (3) substituting ($P_1, T_1$) at ground station level, and ($P_2, T_2$) at the umbrella layer.

Along streamlines with constant $n_i$ compression indices, the sum of the me-

chanical energy components will remain constant [8], used in the conservation Equations (2a) and (2b).

The two-dimensional, time and elevation variation for $P(i,j)=P_i(z_j)$ and $\rho_i(z_j)$ functions can be derived from (3), (4), and the gas law as follows:

$$P(i,j)=P(i,1)\left[\frac{T(i,j)}{T(i,1)}\right]^{\frac{n_i}{n_i-1}} \tag{7}$$

$$\rho(i,j)=\frac{P(i,j)}{RT(i,j)}, \tag{8}$$

where $P(i,1)=Pbar(i)$, and $T(i,1)=T_a(i)$, both expected to be available from the ground-based monitoring station.

The variation of the $P_i(z)$ and $1/\rho_i(z)$ functions are directly related by the $P_i=(\rho_i)^{n_i}=\text{const}$ definition for polytropic compression or expansion.

## 3. The Spontaneous CCE Processes in the Atmosphere

Two possible, simple CCE models are considered which can satisfy the stipulation of net zero vertical mass transport in the TR, excluding the supply of vertical advection in the REV of TR, and allowing only vertical, gradient-driven convection. The two models are: 1) horizontal, but vertically wavy wind, inducing vertical, cell-type mixing of air mass and enhancing vertical, cell-type, CCE thermal exchange; and 2) vertical, thermally-induced expansion-contraction of the mass of air in the TR, enhancing the CCE thermal exchange.

Two other possible cases are postponed for future studies: 3) the large-eddy, statistically homogeneous, dispersion-type, turbulent, vertical mass transport due to the nonzero covariance of the fluctuating density, $\rho'$, and the fluctuating, vertical velocity $w'$, giving a vertical air mass flow exchange by dispersion $\overline{\rho'w'}$, potentially enhancing CCE exchange; and 4) the CCE and other energy transport differences between multiple vertical columns under different cloud and surface vegetation coverage, creating horizontal potential gradients which are still within the same REV of the TR. Horizontal, heat and mass transport branches must be used to connect nodal points in the vertical columns to form closed circuits for horizontal and vertical air flows, self-generating air velocity components that enhance vertical energy transport but without net overall horizontal energy gradients at the outside boundaries of the REV volume. Although the three-dimensional case is expected to be the most general and attractive for applicability, it must be the subject of future work as it requires complex 3D energy and flow transport network model elements. Energy gradient-driven, fluid dynamic simulation is included in air ventilation network flow simulations with the MULTIFLUX code [8] [10] that may be repurposed for case 4) type atmospheric modeling application.

### 3.1. Vertical Transport Cells in the CCE Processes in TR

Two CCE process components are needed to form a Carnot work-heat process in

a vertically stratified TR volume. The two overlapping Carnot processes are shown together Figure 1, one in blue and one in red, in a $p-v$ diagram, where $v=1/\varrho$. A unit mass particle activates the Carnot engine by moving along an $n=n_i$ constant line 1-2 (in blue) for the upper-side expansion route 1-1H-2 and a lower-side compression route 2-2L-1; and the other is an overall compression along 2-1 (in red) for the upper-side compression route 2-1H-1 and a lower-side expansion route 1-2L-2. When overlapped in REV, both CE processes have an upper and a lower side and may transport thermal energy between points 1 and 2 without net air mass exchange and without the need for turbulent dispersion.

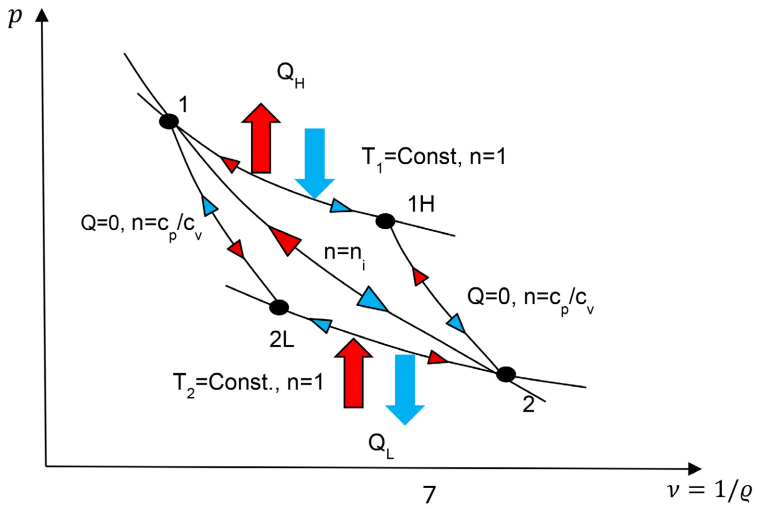


Figure 1. Two Carnot cycle compression-expansion processes shown in red and blue colors between points 1 and 2 along an atmospheric, polytropic trend curve with $n=n_i$ compression index. The thermal energy flow directions are also shown for the counterclockwise (red) and clockwise (blue) circulation directions (after [1]).

The overall compression (in blue) has in series isothermal and adiabatic compression elements on the upper (H) side, and a series adiabatic and of isothermal expansion elements in the lower (L) side. The $Q_H$ (in blue) is the incoming thermal energy to a unit mass lump during 1-2 expansion on the upper side. The $Q_L$ (in blue) is the exiting thermal energy from a unit mass lump during 2-1 compression on the lower side.

In a complete, overall expansion (blue) Carnot cycle, the upper side must gain $Q_H$ thermal energy during 1-2 isothermal expansion and the lower side must lose $Q_L$ thermal energy (both in blue) during 2-1 isothermal compression to a unit mass lump. The area in the 1-1H-2-1 triangle is proportional to $Q_H$ (in blue). The area in the 2-2L-1-2 triangle is proportional to $Q_L$ (in blue). The $Q_H$ and $Q_L$ components are not expected to be equal.

The complete, overall expansion (red) Carnot cycle between 2-1 is the mirror image of that of the previous, overall compression (blue) process; only the signs of the energy terms need to change. The "blue" and "red" processes may not be equally probable in the TR.

The mathematical model of the $Q_H$ and the $Q_L$ thermal energy components for the overall compression process for a discretized vertical column uses the notations $dQ_u$ and $dQ_d$ [J/kg] thermal energy terms for the $Q_H$ and the $Q_L$ components, respectively.

The $dQ_u$ and $dQ_d$ [J/kg] thermal energy terms are calculated from the isothermal processes using (3b) and the $P_{1H}$ and $P_{2L}$ pressures at the mid-points of the upper and lower paths, These pressures are expressed with the help of the adiabatic sections with zero net thermal energy exchange.

The isothermal processes are modeled in the upper and lower sections between point 1 at $(i,j)$ and point 2 at $(i,j+1)$, using the isothermal streamline Equation in (3b). The thermal energy is expressed first from the logarithm of pressures ratio along the isothermal paths, and then the $P_1$, $P_{1H}$ and $P_2$, $P_{2L}$ pressures are expressed with temperatures along the $n_i$ streamline, employing (3) and algebra. The result is obtained in an interesting form, using temperature ratios only on the $n_i = const$ process curve as follows [1]:

$$\begin{aligned} dQ_u(i,j) &= RT(i,j)\ln\left(\frac{P_1}{P_{1H}}\right) \\ &= nI_i \cdot RT(i,j)\ln\left[\frac{T(i,j)}{T(i,j+1)}\right], \ [\mathrm{J/kg}] \end{aligned} \tag{9a}$$

$$\begin{aligned} dQ_d(i,j) &= -RT(i,j+1)\ln\left(\frac{P_{2L}}{P_2}\right) \\ &= -nI_i \cdot RT(i,j+1)\ln\left[\frac{T(i,j)}{T(i,j+1)}\right], \ [\mathrm{J/kg}] \end{aligned} \tag{9b}$$

where

$$nI_i = \frac{n_i}{n_i - 1} - \frac{c_p}{R} \tag{10}$$

The $nI_i$ coefficient may be regarded as the difference of $\frac{n_i}{n_i - 1}$, and $\frac{\kappa}{\kappa - 1}$, where $\kappa = c_p / c_v$, (the adiabatic compression index), as indeed,

$nI_i = \frac{n_i}{n_i - 1} - \frac{\kappa}{\kappa - 1} = \frac{n_i}{n_i - 1} - \frac{c_p}{R}$.

Therefore, if the atmospheric energy transport were adiabatic, the $dQ_u$ and $dQ_d$ terms would be correctly both zero from (9a) and (9b).

### 3.2. Wind-Enhanced, Vertical Thermal Energy Transport by CCE

The thermal energy of $dQ_u$ and $dQ_d$ are in [J/kg] in units, comparable to each other for a constant unit mass of air to satisfy zero net vertical mass transport. Vertical positions change by switching places with no net vertical mass change is conceivable, for example, by crisscrossing vertical positions along the overall, horizontal, average trajectory of air by, e.g., flow over surface waviness [1].

To interpret the CCE terms in (9a) and (9b) for energy conservation in a constant volume, each term at $z(j)$ location must be multiplied by the air density

at the same elevation. To still maintain zero vertical mass balance, the average density must be used as a multiplier, $\bar{\rho}(i,j)=\left(\rho(i,j)+\rho(i,j+1)\right)/2$:

$$dQ_u(i,j)=\bar{\rho}(i,j)\left\{nI_i\cdot RT(i,j)\ln\left[\frac{T(i,j)}{T(i,j+1)}\right]\right\}\ \text{[J/m}^3\text{]} \tag{11a}$$

$$dQ_d(i,j)=-\bar{\rho}(i,j)\left\{nI_i\cdot RT(i,j+1)\ln\left[\frac{T(i,j)}{T(i,j+1)}\right]\right\}\ \text{[J/m}^3\text{]} \tag{11b}$$

The differences between $dQ_u$ and $dQ_d$ thermal energy terms in absolute values are differentially small for fine $dz$ division. The integral values of $dQ_u$ and $dQ_d$ terms are calculated to obtain the total values of CCE energy densities in TR over $Dz$ elevation in [J]. The Rieman summations for the integrals $QCE_u(i)$ and $QCE_d(i)$ are used by taking the scalar product of $\bar{\rho}(i,j)$ and the $dQ_u(i,j)$ and $dQ_d(i,j)$ as vectors, $dz=z_{j+1}-z_j=1$, $dx=dy=1$, for $j\in[1,Dz-1]$:

$$QCE_u(i)=\left\{nI_i\cdot RT(i,j)\ln\left[\frac{T(i,j)}{T(i,j+1)}\right]\right\}\left[\bar{\rho}(i,j)\right]^T\ \text{[J]} \tag{12a}$$

$$QCE_d(i)=\left\{-nI_i\cdot RT(i,j+1)\ln\left[\frac{T(i,j)}{T(i,j+1)}\right]\right\}\left[\bar{\rho}(i,j)\right]^T\ \text{[J]} \tag{12b}$$

The $QCE_u$ and $QCE_d$ energy functions in the single column are depicted from the SCS model for the selected hours in **Figure 2(a)** and **Figure 2(b)** during a fair-weather day, out of a 90-day (2208 hrs) time in a previous study [1]. The CCE components may add or remove thermal energy to or from the single column of volume 1 m × 1 m × *Dz* m. It is assumed that the upward and downward air flow exchange cycles actuates the CCE process over the entire $Dz$ height, separated spatially into cells by the horizontal wind. Note that the exchanges are not necessarily simultaneous, and not in the same vertical, unit-area (1 m × 1 m) column in the large REV volume over a 1 km × 1 km ground wall surface area within 1 hour.

For context to other atmospheric variables, the monitored, hourly air temperatures and the modeled ground wall temperatures are shown in **Figure 3(a)** for the selected hours. The variations of the modeled compression index, $n_i$, and it's modified counterpart from (10), $nI_i$ in TR for the same hours are shown in **Figure 3(b)**. The corresponding compression index for the coldest hour at 7 am ($i=368$ hr) is $n_i=1.2452$, ($nI_i=1.5765$), and for the hottest hour at 4 pm ($i=377$ hr) is $n_i=1.3774$. ($nI_i=0.1482$).

For the effective heat conductivity and thermal diffusivity functions, the heat flux density function over a unit (1 m$^2$) surface area is calculated from one component, e.g., the $QCE_u(i)$ function, as $\left|QCE_u(i)\right|-\left|QCE_d(i)\right|$ is zero within rounding limit:

$$qW_u(i)=\left[QCE_u(i+1)-QCE_u(i)\right]/(1)/3600\ \text{[W/m}^2\text{]} \tag{13a}$$

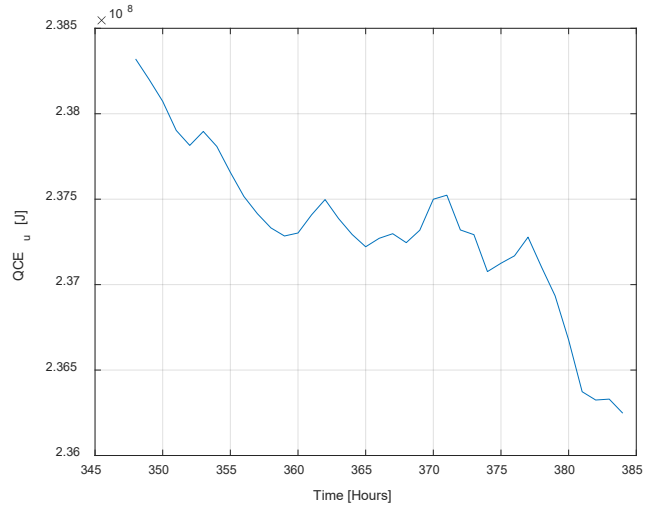


(a)

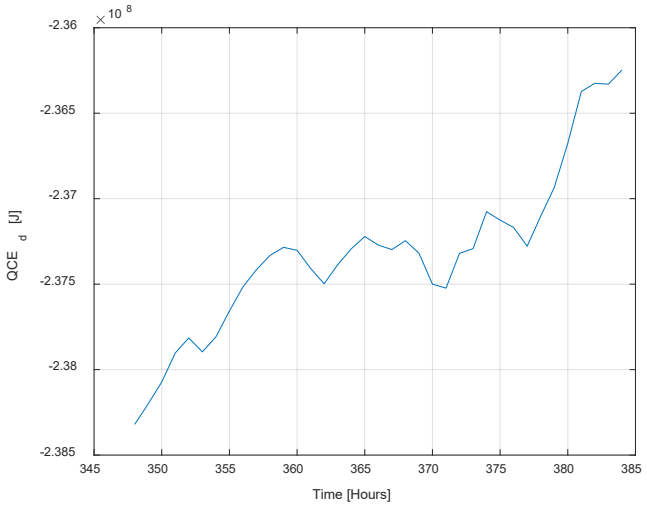


(b)

**Figure 2.** (a) The $QCE_u$ energy function; (b) The $QCE_d$ energy function.

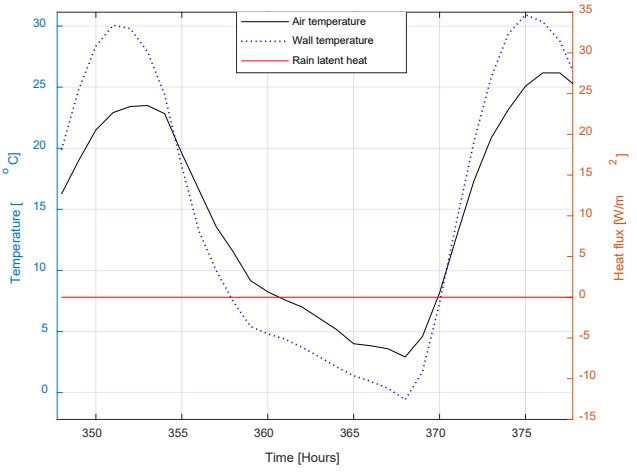


(a)

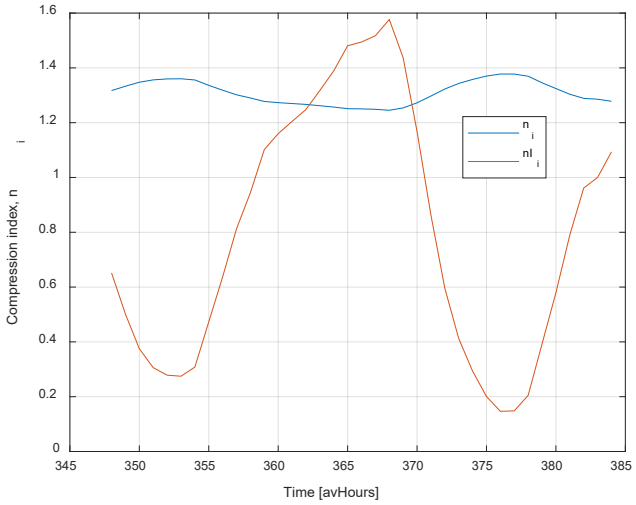


(b)

**Figure 3.** (a) Air and ground wall temperatures; (b) Compression index, $\eta_i$; and $nI_i$, [Equation (10)].

For comparison only, the other component:

$$qW_d(i)=\left[QCE_d(i)-QCE_d(i+1)\right]/(1)/3600 \quad [\mathrm{W/m^2}] \tag{13b}$$

The heat flux density variation with time due to the upward and downward paths in all CCE cells in TR are shown for the selected time period in **Figure 4(a)**, and **Figure 4(b)**, respectively.

The effective thermal conductivity of $k_{eff}(i)$ in the TR is evaluated from the defining equation of $qW(i)=k_{eff}(i)\cdot dTa(i)/dz=k_{eff}(i)\cdot alr(i)$:

$$k_{eff}(i)=\left|qW(i)\right|/alr(i) \quad [\mathrm{W/m/K}] \tag{14}$$

The dispersity coefficient $D(i)$ is calculated from the defining equation of:

$$D(i)=k_{eff}(i)/Cp(i)/\overline{\rho}(i),\ [\mathrm{m^2/s}] \tag{15}$$

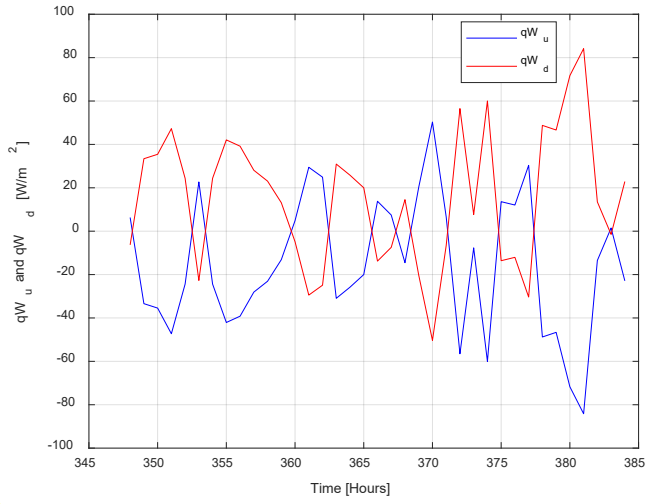


(a)

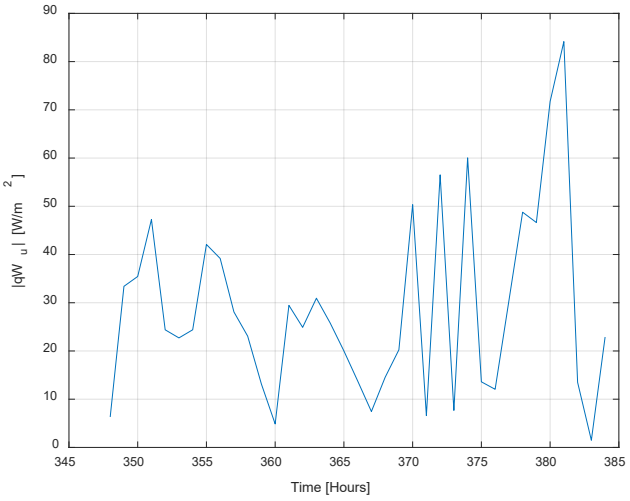


(b)

**Figure 4.** (a), $qW_u$ and $qW_d$ components together from CCE; (b), $|qW_u|$ to represent CCE in TR.

where $alr(i)$, $Cp(i)$, and $\bar{\rho}(i)$ are the lapse rate, specific heat, and average density, respectively, at time index $i$ in the TR.

The effective heat conductivity and the thermal dispersity coefficient are shown in **Figure 5(a)**, and **Figure 5(b)**, respectively for a single, but simultaneous CCE event in each hour along the single column in TR.

It is helpful to recall the thermodynamic energy balance for closed work cycles, such as in the upper and lower closed triangles in **Figure 1**, explained in the foregoing. It is stated in the art that the total thermal energy terms must be equal to the mechanical energy terms in closed cycles [11]. Without re-proving with algebra, the total thermodynamic energy terms are written for the TR, adding the extra thermal terms to those in the mechanical components in (1):

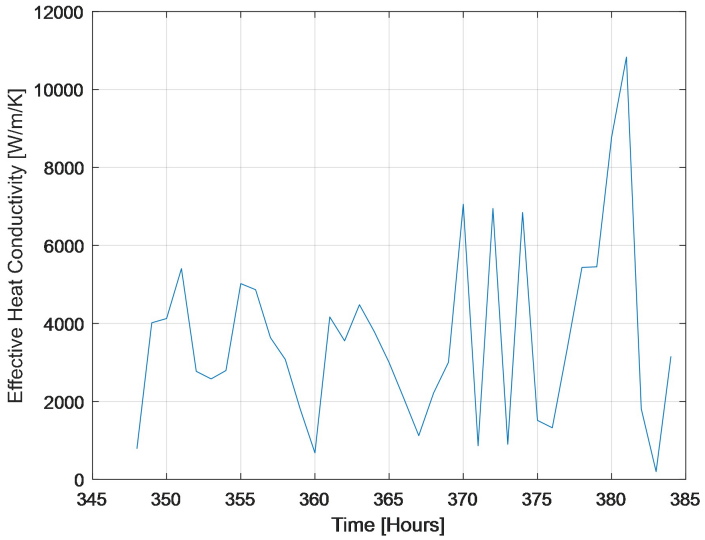


(a)

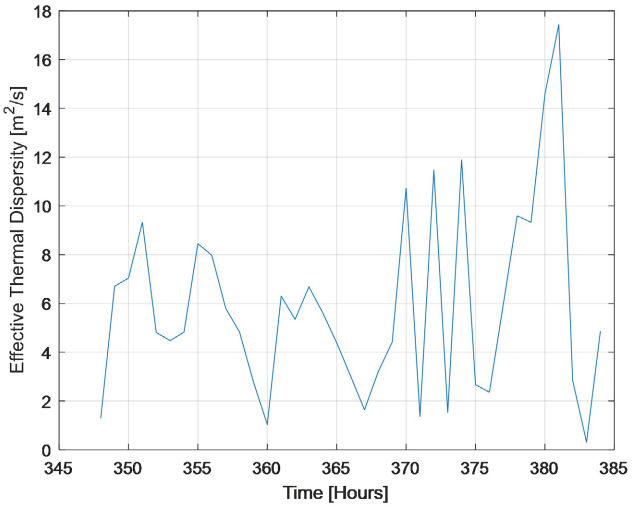


(b)

**Figure 5.** (a) Heat conductivity from one CCE/hr event; (b) Thermal Dispersity from one CCE/hr.

$$d\left(\frac{P}{\rho}+g\cdot z+\frac{v^2}{2}+C_v\cdot T\right)=d\left(W_s-W_\tau\right)+d\left(Q_h+Q_\tau\right), \tag{16}$$

Recollect that the $W_s-W_\tau$ term is included as a positive turbulent energy input of the wind by initial estimation and correction. The $W_s-W_\tau$ is removed to the left side in the hydrostatic law in (5) for combining it with the gravitational constant as a "hydrostatic defect" for resolving $P(z)$ with elevation in TR, and eliminating this mechanical term by dissolving it in the compression index via $(P_1,T_1)$, and $(P_2,T_2)$ where 1 is surface and 2 is upper, umbrella edge location. The $Q_h$ and $Q_\tau$ are the added (or removed) thermal energy, and friction heat from $W$, respectively. The TR is an energy-balanced system, defined by H1, H2, T1 and T2. If the energy system absorbs $W_s-W_\tau$ in TR via $n$, and $W_\tau=Q_\tau$, then $Q_\tau$ must be added to the thermal energy balance in the total TD equation. For a well-balanced weather system with no trade wind, $W_\tau$ may be estimated to be $W_\tau=W_s/2$.

Combining (2) with (13), incorporating $W_s$ into $n$, and bringing the previously discarded thermal CCE term as heat from the mechanical energy balance to the right side, and assuming the practical case of $n\neq 1$ gives the full thermodynamic conservation equation:

$$d\left[\left(\frac{n}{n-1}\right)R\cdot T+g\cdot z+\frac{v^2}{2}\right]=d\left[\left(\frac{1}{n-1}\right)R\cdot T-C_v\cdot T+Q_h+Q_\tau\right] \text{ for } n\neq 1 \tag{17}$$

The left side of (17) is considered to be equal to the sum of the $dQ_u(i,j)$ and $dQ_d(i,j)$ terms defined by (9a) and (9b) for [J/kg] units, as $v=0$ for the vertical advection velocity component in TR.

For the specific energy in unit volume in [J/m$^3$], (17) must be multiplied with mean value of the air densities at their entering points for mass conservation between the upper and the lower triangles in CCE. For this case, the $dQ_u(i,j)$ and $dQ_d(i,j)$ terms are defined by (11a) and (11b) for [J/m$^3$] units.

### 3.3. Solar-Driven, Temperature- and Pressure-Enhanced, Vertical Energy Transport by CCE

The ground wall surface temperature varies by seconds from periodical, diurnal solar irradiation heating, and nocturnal infrared radiation cooling. The air temperature field follows course in TR, measurable by weather stations close to the ground wall and resolved from the SCS model giving a time- and elevation-dependent temperature and pressure fields. Due to thermal expansion and contraction, two processes are in play: 1) the air density changes with elevation and time; and 2) the elevations of the center of gravity of the expanding mass elements in each pixel change with time, relative to the fixed vertical coordinates of $z$ in TR.

A straightforward way to model the elevation change for each pixel and integrate them over elevation is to calculate the change in the elevation of the center of gravity of the TR, $z_{cgTR}$, due to air density change in a changed temperature and pressure field, varying in time.

The $z_{cgTR}(i)$ is numerically calculated in SCS as the first moment of the density function $\rho(i,j)$ over elevation $z(j)$;

$$z_{cgTR}(i)=\left[\sum_{j=1}^{Dz} z(j)\rho(i,j)\right]\Big/\sum_{j=1}^{Dz}\rho(i,j) \tag{18}$$

The vertical velocity of $z_{cgTR}$ within each hour at time index $i$ is written as a finite differential:

$$v_{cgTR}(i)=\left[z_{cgTR}(i+1)-z_{cgTR}(i)\right]/3600,\ [\mathrm{m/s}] \tag{19}$$

The $qCE_{vcg}(i)$ energy transported by the CCE process at every hour in the TR is calculated from the column-averaged values of the $qCE_u(i)$ and $qCE_d(i)$ terms of (11a) and (11b), expressed from (12a) and (12b) as follows:

$$\overline{qCE_u}(i)=\left\{nI_i\cdot RT(i,j)\ln\left[\frac{T(i,j)}{T(i,j+1)}\right]\right\}\left[\bar{\rho}(i,j)\right]^T/(1)/Dz \quad [\mathrm{J/m^3}] \tag{20a}$$

$$\overline{qCE_d}(i)=\left\{-nI_i\cdot RT(i,j+1)\ln\left[\frac{T(i,j)}{T(i,j+1)}\right]\right\}\left[\bar{\rho}(i,j)\right]^T/(1)/Dz \quad \{\mathrm{J/m^3}] \tag{20b}$$

The rate of energy density is calculated from the column-averaged $\overline{qCE_u}(i)$ and $\overline{qCE_d}(i)$ values by selectively multiplying each by the $v_{cgTR}(i)$ velocity component, according to the vertical flow direction:

$$qCE_{vcg}(i)=\begin{cases} v_{cgTR}(i)\cdot\overline{qCE_u}(i), & \text{if } v_{cgTR}(i)>0 \\ -v_{cgTR}(i)\cdot\overline{qCE_d}(i), & \text{if } v_{cgTR}(i)\le 0 \end{cases} \quad [\mathrm{W/m^2}] \tag{20}$$

Effective heat conductivity and thermal dispersity functions are calculated as before.

The $v_{cgTR}$ velocity and $qCE_{vcg}$ rate of energy density (power) in 1 m × 1 m × Dz [m] single column are shown in **Figure 6(a)**, and **Figure 6(b)**, respectively. The effective heat conductivity, driven by the variation of air density, and the corresponding, effective thermal dispersity are shown in **Figure 7(a)** and **Figure 7(b)**, respectively.

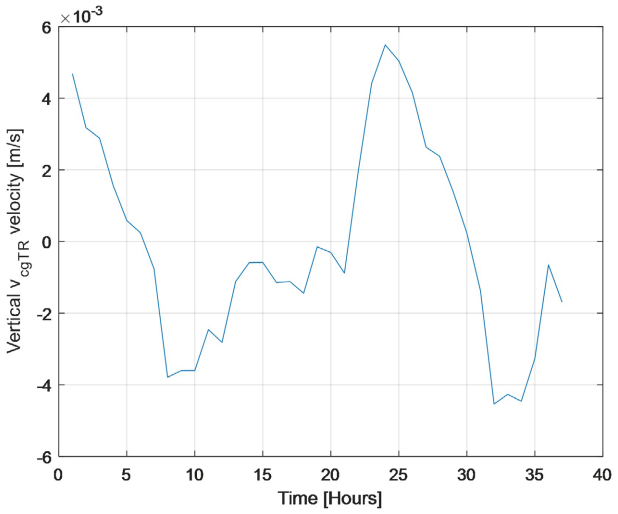


(a)

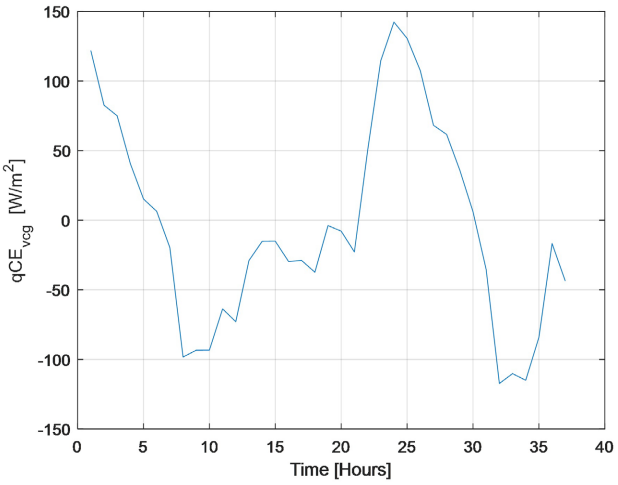


(b)

**Figure 6.** (a). Average, vertical uplift velocity in TR; (b) The up or down CCE power in TR.

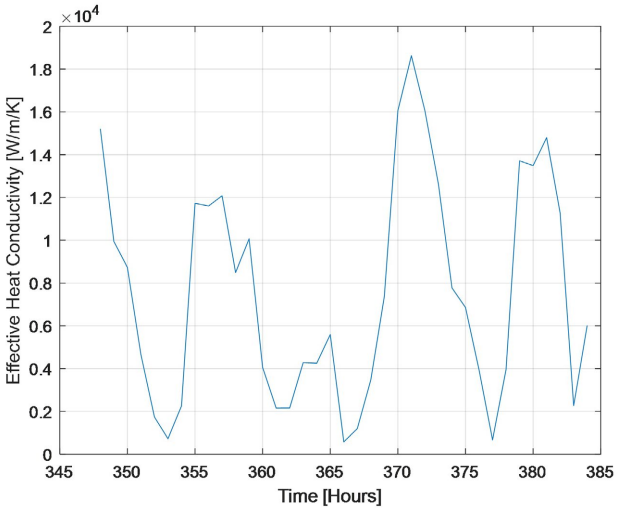


(a)

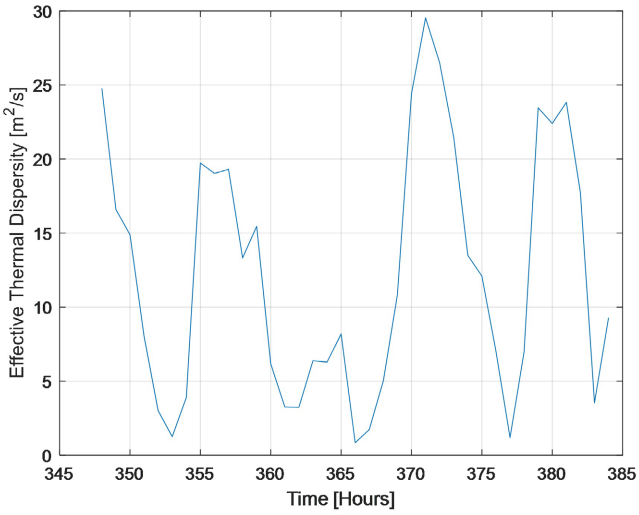


(b)

**Figure 7.** (a) Effective heat conductivity from air density variation; (b) Effective thermal dispersity.

## 4. Discussions

As defined in the example, a REV of $10^7$ $m^3$ in a TR zone is under gravity and vertically stratified temperature and air pressure fields, with 10 million air-filled, $1m^3$ cells. Each of these cells is pictured as a host of two overlapped CEE cells, both may be dormant or activated. Once enhanced by the temporal change in solar and other radiation heat source, or by the horizontal wind with an always present vertical component, a large potential opens to move thermal energy in vertical direction. The CCE-generated vertical rate of energy can keep the atmosphere in balance thermodynamically at every second, by complying with the dynamically changing, vertical temperature lapse rate.

Wind-driven, vertical crisscrossing of air pockets between equivalent, neighboring vertical columns actuates vertical, compression-expansion thermal energy transport, while changing no net air mass vertically. The potential is shown in **Figure 5(a)** and **Figure 5(b)** for one single column's CEE cell's thermal transport capacity in both effective heat conductivity [W/m/K] and thermal dispersity [$m^2/s$] from a single instant of one full vertical mixing exchange in each hour. The result in **Figure 5(a)** for heat conductivity is comparable to superconductors, due to the very low temperature gradient in TR that is in the denominator in (13). Thermal dispersity values in **Figure 5(b)** are only about 5 - 10 times higher than reported values for mid-TR elevation of the atmospheric air. The potential heat transport is from a single-instant CCE cycle in one hour. The effective heat conductivity and thermal dispersity are both proportional to the rate of CCE cycle repetitions.

Further study is needed to estimate the cycle repetition rate for an accompanying enhancement multiplier for vertical heat transport, and to verify the availability of wind capacity for at least one CCE cycle per hour for realizing the outcomes shown in **Figure 2**, **Figure 4**, and **Figure 5**.

### 4.1. Discussion of Horizontally Driven, Wind-Enhanced qCE Transport

The sum of the upper and lower components, $qCE_u(i)+qCE_d(i)$ may be close to zero at every time index, but their individual paths work intensively as shown in Figure 4 and Figure 5 for a single CCE cycle incident in one hour in each 1 m vertical section in the TR volume. With a horizontal, 2 m/s average air velocity in the example over a 3-month period, millions of CCE cycle incidents may happen. The potential may be estimated by an accompanying function from the RMS of the large-eddy variations of the vertical velocity component of the wind velocity, of which only the horizontal component is reported routinely.

As recalled from [1], a horizontal, stochastically or chaotically varying wind may cross the REV horizontally over a level ground but may change elevation of the streamlines along the travel over surface perturbations while statistically satisfying mass conservation at every elevation in a finite, e.g. 5 min or 1 hour, time interval. Individual Carnot cycles may be driven by the elevation change, along the crisscrossing horizontal wind patterns and creating virtual, irrotational vortices. If horizontal layers travel not parallel as $\begin{bmatrix} 2 & \rightarrow & 2 \\ 1 & \rightarrow & 1 \end{bmatrix}$ but stochastically or chaotically crisscross as $\begin{bmatrix} 2 & \searrow & 1 \\ 1 & \nearrow & 2 \end{bmatrix}$ in each $dz = 1$ [m] pixels as a mixing instant, the result is mixing the vertical, (2, 1) order into (1, 2) order without rotating the pixel. Shifting the position of the $1 \times 1$ [m] column by $dx = vdt$ horizontal distance within the REV's surface boundaries that may be 10 km × 10 km is still within the averag domain of the SCS model. The lack of experimental results in the literature is surprising about direct measurements of low-frequency variations of vertical wind velocity components.

### 4.2. Discussion of the Solar-Driven Vertical Pulsation Enhancement of the qCE Transport

The ground wall surface temperature varies by seconds from periodical, diurnal solar irradiation heating, and nocturnal infrared radiation cooling. The air temperature field follows course in TR, measurable by weather stations close to the ground wall and resolved from the SCS model giving a time- and elevation-dependent temperature field. Due to thermal expansion and contraction, two processes are in play: 1) the air density changes with elevation and with time [(already modeled in the $dQ_u$ and $dQ_d$ terms in (11a) and (11b)]; and 2) the elevations of the center of gravity of the expanding mass elements in each pixel change with time, relative to the fixed vertical coordinates of $z$ in TR.

A straightforward way to model the elevation change for each pixel and integrate them over elevation is to calculate the change in the elevation of the center of gravity of the TR due to air density change in a changed temperature and pressure field, varying with time.

As shown in Figure 6(a), and Figure 6(b), the vertical air velocity and the rate of energy density (power) are low-frequency functions with time. The thermal energy transport measured in effective heat conductivity is higher that of the wind-enhanced CCE value, for a single CCE cycle in one hour in a full, 1 m × 1 m × Dz [m] air column. The extremally high effective heat conductivity means that the atmospheric air will vigorously seek to comply with the linear temperature distribution between points 1 and 2 in two different elevations, that is, in the single column example, between surface and the top of TR.

## 5. Conclusions

Vertical, convective, thermal energy transport is examined with the Carnot process and the compressible energy dynamics model that is simple for explanation and needs little computational resources.

The recently discovered Carnot Compression-Expansion (CCE) cells [1] by creative imagination are modeled and proven in the present study in Point 3.3 by energy balancing exercise in the stratified atmosphere by gravity, and the vertical gradients of pressure, temperature, and density. The CCE cells can be activated by natural weather processes.

The mixing-driving capacity of the horizontal wind is found to be a likely cause to experience significant vertical energy transport in TR. However, the wind's statistically random or even stochastic nature makes this component difficult to predict and its effects resolved in a numerical predictive model. Further research is needed to resolve this component by direct measurement.

The driver of the thermal expansion and contraction of the troposphere by periodic solar heating and self-radiation cooling of the ground is a reliable and predictable component, and a cause of CCE activation. This case shows strong and promising vertical energy transport in the troposphere, even without horizontal wind enhancement.

Combining the two different enhancement processes by superposition as parallel events is readily feasible.

Resolving the accompanying function for CCE cycles repetitions is a future task to explore the full potential of vertical transport by CCE processes in the atmosphere.

The spatially uneven heating and cooling effects from surface and cloud variations can be conveniently analyzed with a single-column system if no net horizontal, mesoscale driving gradients are present.

## Acknowledgements

My spouse, Emoke is thankfully acknowledged for her support and patience during the preparation of the manuscript.

## Conflicts of Interest

No conflicts are to be reported.

## References


[1] Danko, G. (2025) Atmospheric Process Model with Energy Dynamics Transport Network Analysis. *Applied Mathematics*, **16**, 535-583. https://doi.org/10.4236/am.2025.167031

[2] Alinot, C. and Masson, C. (2005) K-E Model for the Atmospheric Boundary Layer under Various Thermal Stratifications. *Journal of Solar Energy Engineering*, **127**, 438-443. https://doi.org/10.1115/1.2035704

[3] Blocken, B., Stathopoulos, T. and Carmeliet, J. (2007) CFD Simulation of the Atmospheric Boundary Layer: Wall Function Problems. *Atmospheric Environment*, **41**, 238-252. https://doi.org/10.1016/j.atmosenv.2006.08.019

[4] Foken, T. (2006) 50 Years of the Monin-Obukhov Similarity Theory. *Boundary-Layer Meteorology*, **119**, 431-447. https://doi.org/10.1007/s10546-006-9048-6

[5] Monin, A.S. and Obukhov, A.M. (1954) Basic Laws of Turbulent Mixing in the Surface Layer of the Atmosphere. *Contributions of the Geophysical Institute of the Slovak Academy of Sciences*, **24**, 163-187.

[6] Obukhov, A.M. (1971) Turbulence in an Atmosphere with a Non-Uniform Temperature. *Boundary-Layer Meteorology*, **2**, 7-29. https://doi.org/10.1007/bf00718085

[7] Stiperski, I. and Calaf, M. (2023) Generalizing Monin-Obukhov Similarity Theory (1954) for Complex Atmospheric Turbulence. *Physical Review Letters*, **130**, Article ID: 124001. https://doi.org/10.1103/physrevlett.130.124001

[8] Danko, G. (2016) Model Elements and Network Solutions of Heat, Mass and Momentum Transport Processes. Springer-Verlag, 1-251.

[9] Dutton, J.A. (1973) The Global Thermodynamics of Atmospheric Motion. *Tellus*, **25**, 89-110. https://doi.org/10.1111/j.2153-3490.1973.tb01599.x

[10] Danko, G., Bahrami, D. and Stewart, C. (2020) Applications and Verification of a Computational Energy Dynamics Model for Mine Climate Simulations. *International Journal of Mining Science and Technology*, **30**, 483-493. https://doi.org/10.1016/j.ijmst.2020.03.019

[11] Welty, J.R., Wicks, C.E., Wilson, R.E. and Rorrer, G.L. (2007) Fundamentals of Momentum, Heat, and Mass Transfer. 5th Edition, Wiley, 740 p.